EUROPEAN ORGANIZATION FOR NUCLEAR RESEARCH
European Laboratory for Particle Physics

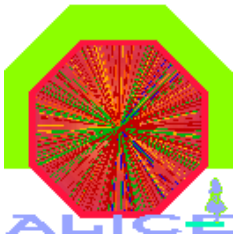

Internal Note/Forward Detector/V0
ALICE reference number
ALICE-INT-2006-018 version 1.0
Date of last change
14.09.2006

Simulation of the V0A Detector

Authors:

J.R. Alfaro Molina[3] E. Belmont Moreno[3] E. Cuautle[3]
I. Domínguez[3] A. Gago[2] G. Herrera Corral[1] A. Flores[3]
V. Grabski[3] M.I. Martínez[3] A. Martínez Dávalos[3]
A. Menchaca Rocha[3] L.M. Montaño Zetina[1] L. Nellen[3]
C.E. Prez[2] A. Sandoval[3]

[1] Centro de Investigación y de Estudios Avanzados, Dpto. de Física, Dpto. de Física Aplicada.
[2] Pontificia Universidad Católica del Perú, Dpto. de Ciencias, Sección Física.
[3] Universidad Nacional Autónoma de México, Inst. de Ciencias Nucleares, Inst. de Física.

Abstract:

The V0A detector is one of the forward detectors that will be used for level zero trigger in the ALICE experiment at CERN. The simulation of the optical response of the V0A elements are presented in this work, which is based on the LITRANI package modified to include wavelength shifting fibers. The simulation indicates a flat response of the whole detector as well as an efficient signal at the output.

Simulation of the V0A Detector

J.R. Alfaro Molina[3] E. Belmont Moreno[3] E. Cuautle[3]
I. Domínguez[3] A. Gago[2] G. Herrera Corral[1] A. Flores[3]
V. Grabski[3] M.I. Martínez[3] A. Martínez Dávalos[3]
A. Menchaca Rocha[3] L.M. Montaño Zetina[1] L. Nellen[3]
C.E. Pérez[2] A. Sandoval[3]

[1] Centro de Investigación y de Estudios Avanzados, Dpto. de Física, Dpto. de Física Aplicada.

[2] Pontificia Universidad Católica del Perú, Dpto. de Ciencias, Sección Física.

[3] Universidad Nacional Autónoma de México, Inst. de Ciencias Nucleares, Inst. de Física.

Abstract

The V0A detector is one of the forward detectors that will be used for level zero trigger in the ALICE experiment at CERN. The simulation of the optical response of the V0A elements are presented in this work, which is based on the LITRANI package modified to include wavelength shifting fibers. The simulation indicate a flat response of the whole detector as well as an efficient signal at the output.

1 Introduction

The V0A detector is part of a system which consists of two arrays of scintillator cells forming discs and installed, concentric to the beam direction, on both sides of the ALICE interaction point. The system will provide online signals for the level zero trigger in both proton-proton and ion-ion collisions. Our analysis will be mainly based on the description of the ALICE V0A detector given in the Technical Design Report [1].

The simulation of the detector response is important because it allows not only to check the resolution and homogeneity of the detector but also to have an estimate of the number of photons hitting the photomultiplier tube (PMT). This is also important because it provides an important tool for testing any unexpected change in the manufacture of the detector.

We have used the LITRANI [2] package. This is a general purpose Monte-Carlo software to simulate the propagation of optical photons in any material. It is written in C++ and was originally developed for the calibration of the CMS calorimeter.

We have developed the code using the version v3.0 of LITRANI in a Root [3] v4.08f framework. Our goals in this report are to describe the response of each isolated cell of the disk and as a whole, varying the number of wavelength shifting (WLS) fibers and their

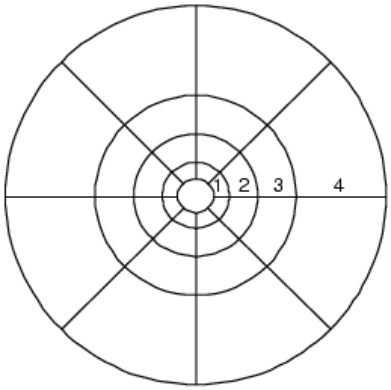

Figure 1: Construction of V0A disc. The cells are numerated from 1 to 4 according to their pseudorapidity coverage.

position within the cells. To be able to fulfill that, we had to include the WLS effect into the LITRANI package including as well the time response.

Our aims have been the following:

- analysis of the optimal position and number of wavelength fibers in the scintillating cell,
- analysis of the homogeneity in each cell of the detector,
- analysis of the homogeneity in the entire detector,
- propagation of photons through the wavelength shifting fibers,
- estimation of the photomultiplier signal.

2 Setup

2.1 Geometry

The V0A scintillator disc has a thickness of 2.5cm and is subdivided in eight sectors of 45 degrees. Each sector is composed by 4 isolated cells (circular sector prisms) as shown in figure 1. The dimensions of this cells are characterized by the following radii: 4.2cm, 7.6cm, 13.8cm, 22.7cm, 41.3cm. WLS fibers are embedded in each cell as shown in figure 2. Note that there is an air gap between the plastic scintillator and the WLS fibers in order to guarantee a better transmission to the PMT. This geometry was adopted for ease of simulation; in reality, the fibers and groves have a circular shape.

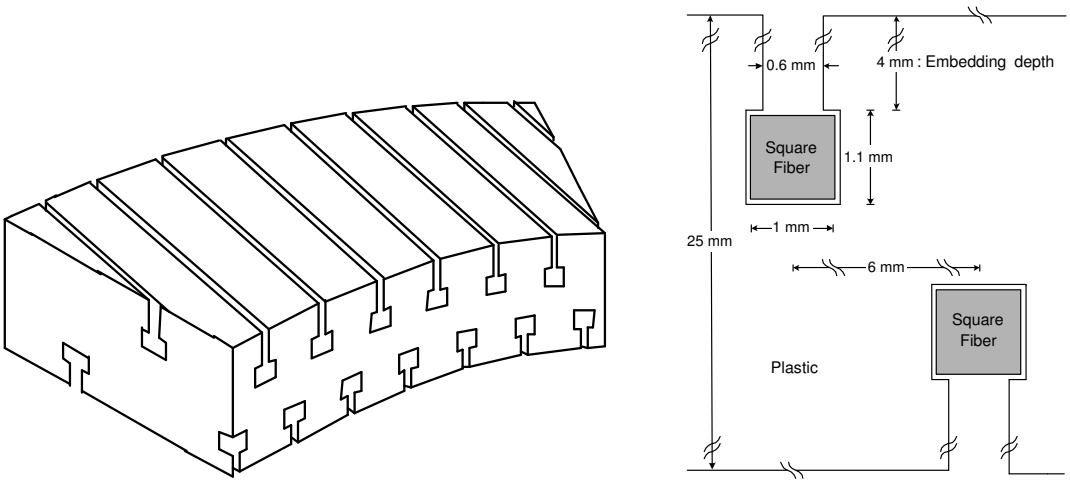

Figure 2: The square fibers are embedded in the plastic leaving an air gap between each fiber and the plastic. Left, geometrical definition of a cell; right, embedding dimensions.

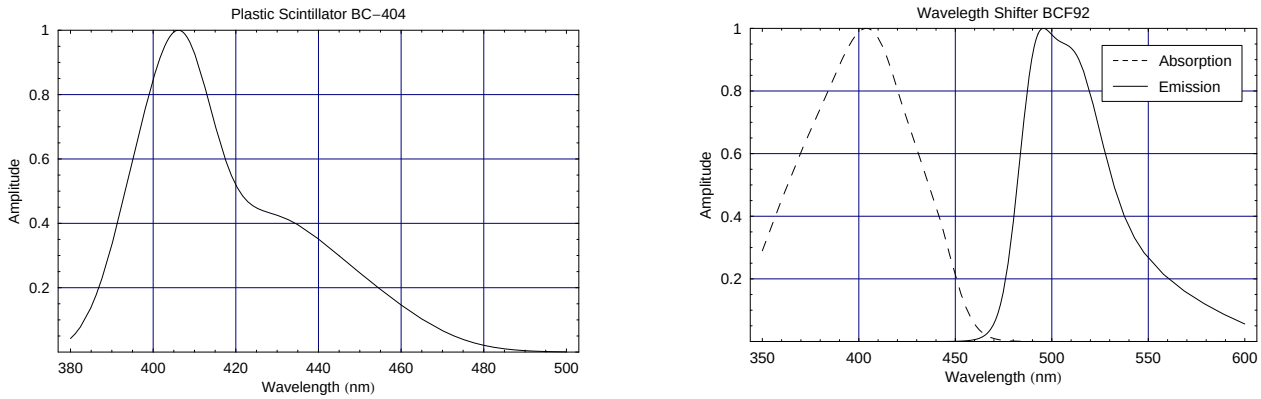

Figure 3: Emission spectrum of BC404 (left plot), and absorption and emission spectrum of BCF92 (right plot), as extracted from reference [4].

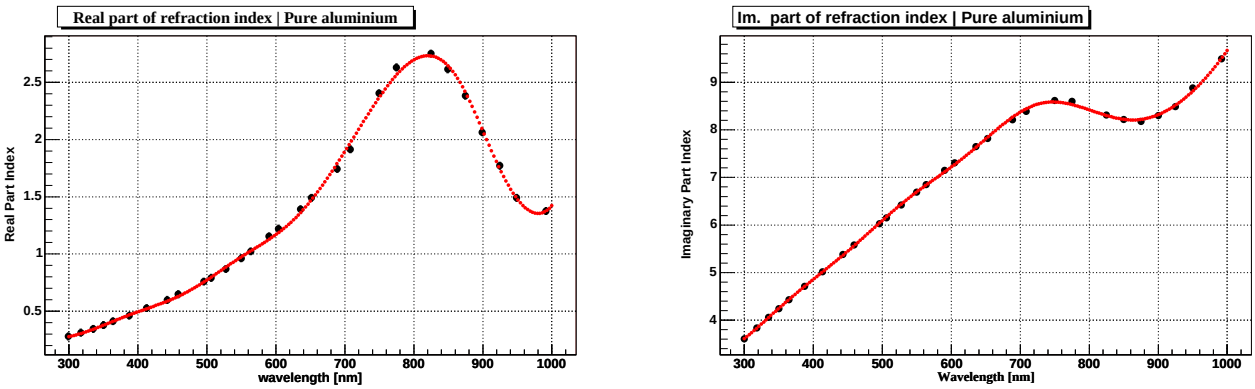

Figure 4: Real and imaginary part of the refractive index of the aluminum wrapping. Values extracted from LITRANI [2].

2.2 Materials

The plastic scintillator (BC404) and the WLS fibers (BCF92) characteristics were taken from the corresponding Bicron datasheet [4]. For the characterization of light generation and transport we use the following parameters:

Plastic scintillator

- Absorption length: 160cm
- Refraction index: 1.58
- Decay time: 1.8ns
- Energy deposition: 2.5 MeV/cm [1]
- Light output: 10200 ph/MeV [2]

Wavelength shifting fibers

- Absorption length: 400cm
- Refraction index: 1.58
- Decay time: 0.85ns

The optical response of these two elements are shown in figure 3. Each cell is covered with an aluminum wrapping using LITRANI parametrization for this material (See figure 4).

2.3 Beam

We use pions of 6.5 GeV fired along the z axis (according to ALICE Coordinate System) with random positions in a rectangle defined in two ways:

- Beam 1: For a complete illumination of the cell, the rectangle covers the entire cell as shown in figure 5 where one hundred pions are fired randomly. This kind of beam has

[1] Value extracted from reference [5]
[2] Value computed from 68% anthracene according to reference [6]

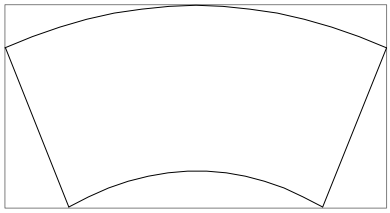

Figure 5: Region of random generation for pion positions.

been used for testing the response of the whole cell when varying parameters related to the geometry.

- Beam 2: The above area is sub divided in 70x70 rectangles. Ten pions are fired in each rectangle. The uniformity of the beam is very important, because in this way any region, within a particular cell, can be treated in equal manner.

The reason to use 6.5 GeV pions lies on the fact that this beam was used at T10 tests during design. Though we do not make a comparison with experimental results here, the beam test measurements do agree with the expected flat efficiency of the simulations. Furthermore, the energy deposition for pions has a plateau for energies from 6 GeV to 1 TeV, so we do not expect a big change on the light production as we go to higher energies.

3 Cell Analysis

3.1 Acceptance of fibers

Many tests have been done embedding fibers in the plastic. This technique has proved to be a good method to collect light from the scintillator. However, to get an optimal collection of light, it is neccesary to test different changes in several design parameters of the scintillation cell. The number of WLS fibers is one of these parameters as well as the depth of embedding, keeping fixed the disk thickness at 2.5cm. In this part of the analysis, we are interested only in the photons that are collected by the fibers.

3.1.1 Efficiency

When a 6.5 GeV pion hits the plastic it generates 63 750 photons typically. Some of them are absorbed and get lost before they reach the optical fiber. We define "efficiency" as the ratio between collected and produced photons.

One can plot the efficiency for each point of the cell as it is shown in figures 6 and 7. This geometric efficiency shows the uniformity of detection. As one can see, the efficiency in each cell varies from 0.40 to 0.55, approximately. We can see that the zones which present a larger efficiency are located in the upper corners of the cells, probably due to the reflections from the sides.

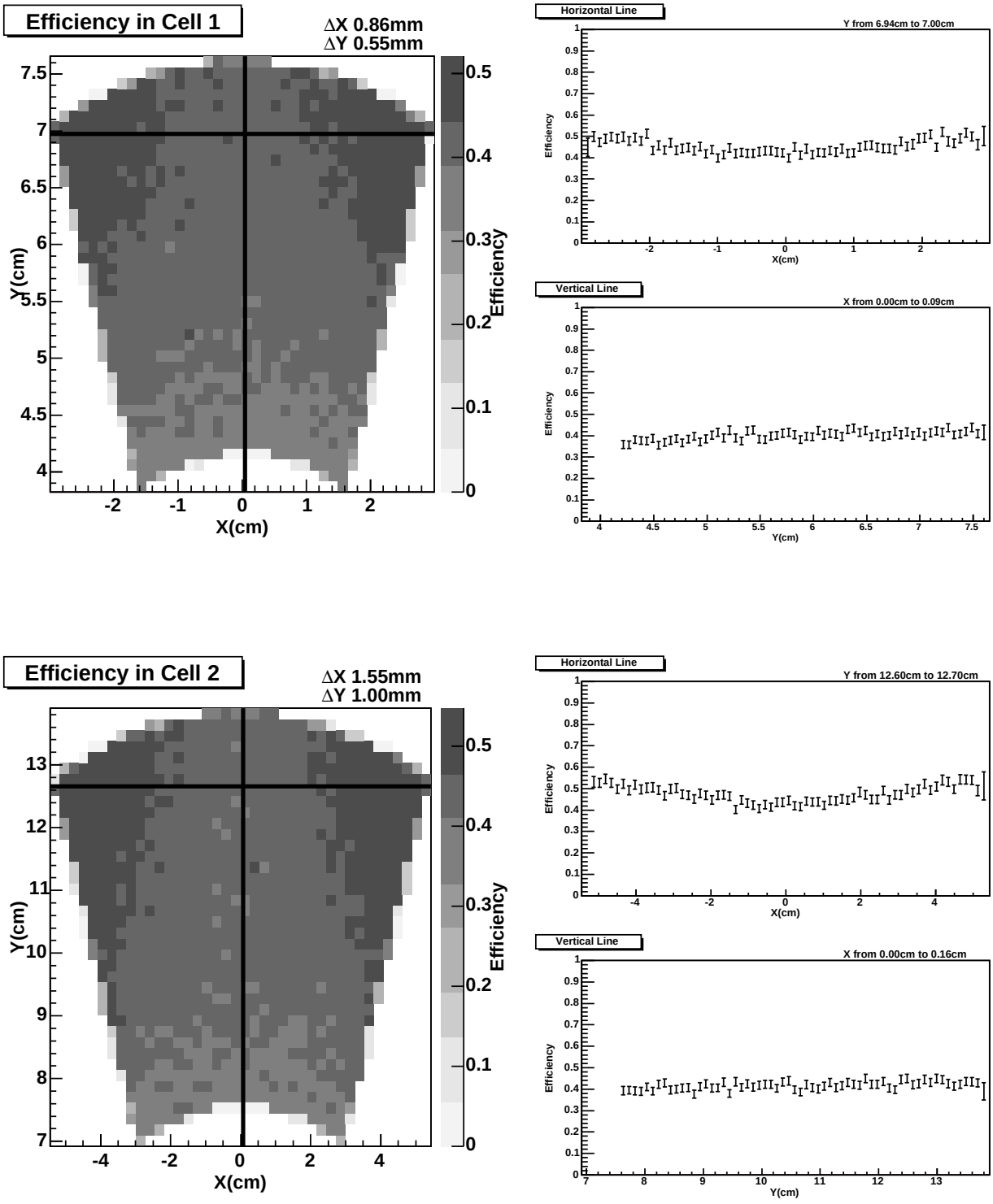

Figure 6: Geometrical efficiency in the first and second cells. Left: Geometrical efficiency. Right: Efficiency along the horizontal and vertical lines (shown on the left) with one bin width.

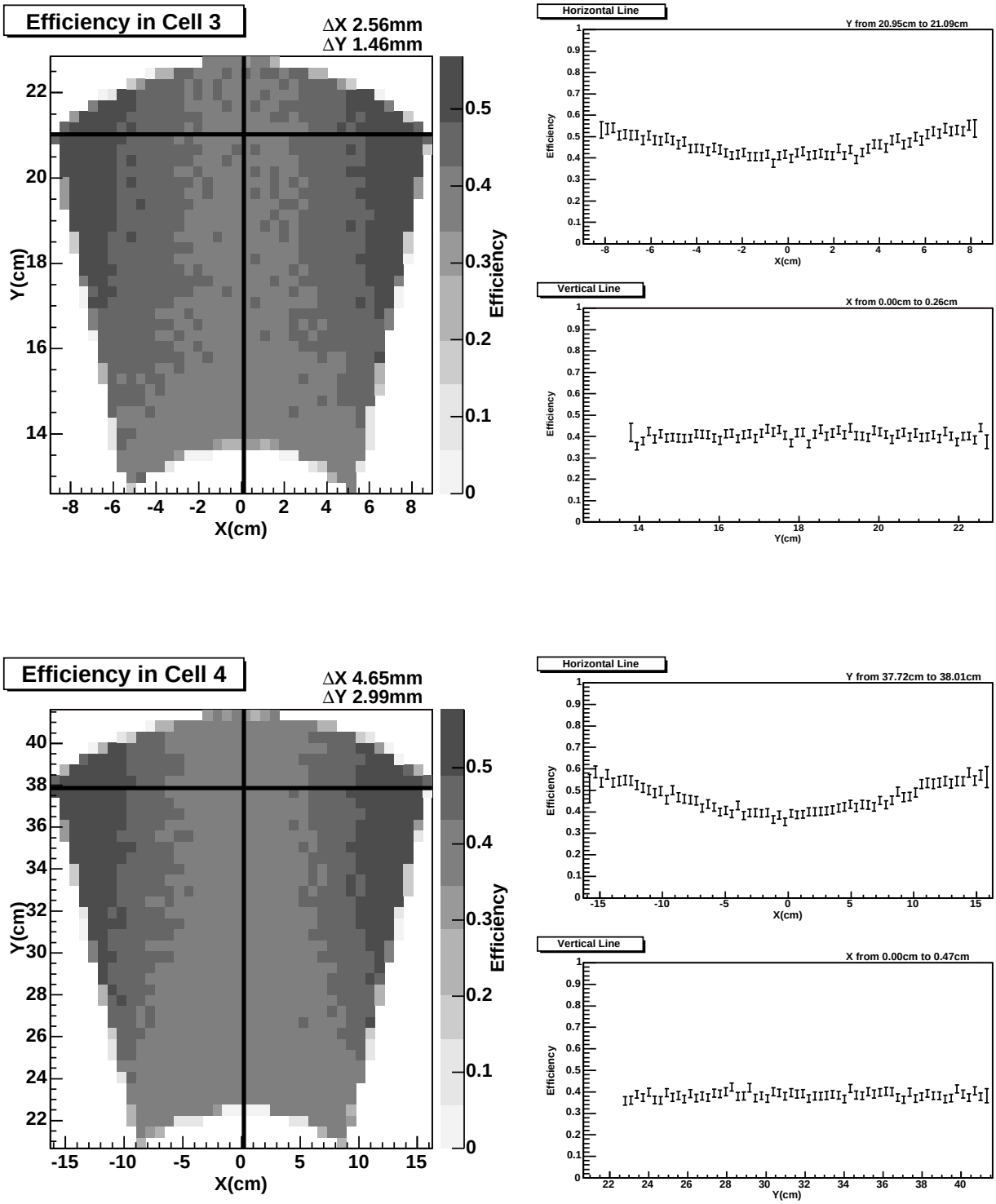

Figure 7: Geometrical efficiency in the third and fourth cells. Left: Geometrical efficiency. Right: Efficiency along the horizontal and vertical lines (shown on the left) with one bin width.

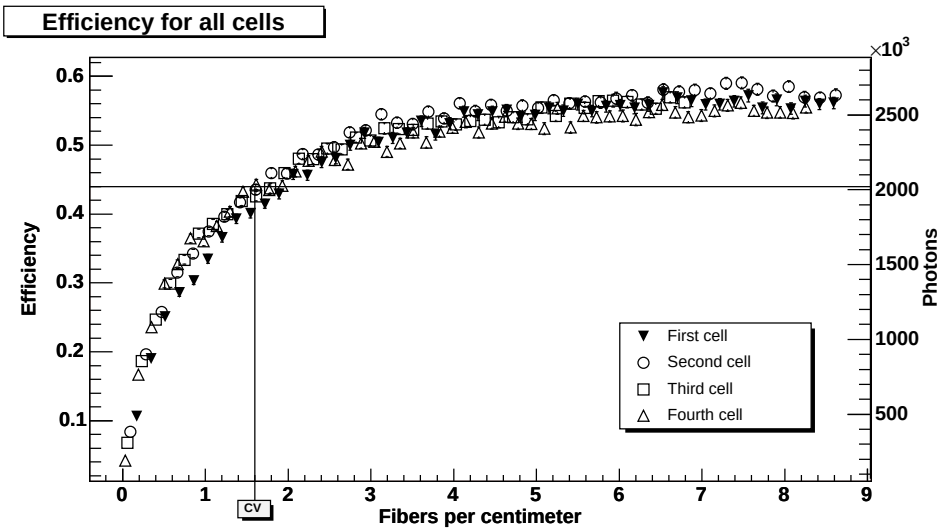

Figure 8: Efficiency vs number of fibers per centimeter for beam 1. The right axis correspond to the mean number of photons collected by the fibers.

In the right side of figures 6 and 7, we show the geometrical efficiency for two lines as well as the gaussian statistical error due to the number of photons generated.

3.1.2 Efficiency dependence upon the number of fibers

In Figure 8, we show the efficiency versus the number of fibers per centimeter. We have the same behaviour for the efficiency of the four cells. This analysis helps us to select the number of fibers per cell, in order to get a homogeneous geometrical efficiency for the whole disk. From the figure, we can see that a density of 1.6 fibers per centimeter, which is the current value (CV), corresponds to 10, 18, 29 and 53 for the first, second, third, and fourth cell, respectively. With this value, we have an optimal cost to benefit ratio, i.e. increasing the density of fibres from say 1.6 to 2 would mean increasing the number of fibers up to 11 more for the fourth cell, while the efficiency would only increase from 0.44 to 0.46.

It is important to say that figure 8 shows a flat efficiency over the whole V0A disc, i.e. the efficiency would be approximately the same in all the cells. We use a function to parametrize the efficiency:

$$\mathrm{Eff}(x) = 0.551(1 - 0.903e^{-0.962x}) \quad , \tag{1}$$

where x is the number of fibers per centimeter.

It is important to note that in figure 8 we are extending the scale of number of fibers until a very large (unrealistic) amount, because we are interested in showing the saturating effect.

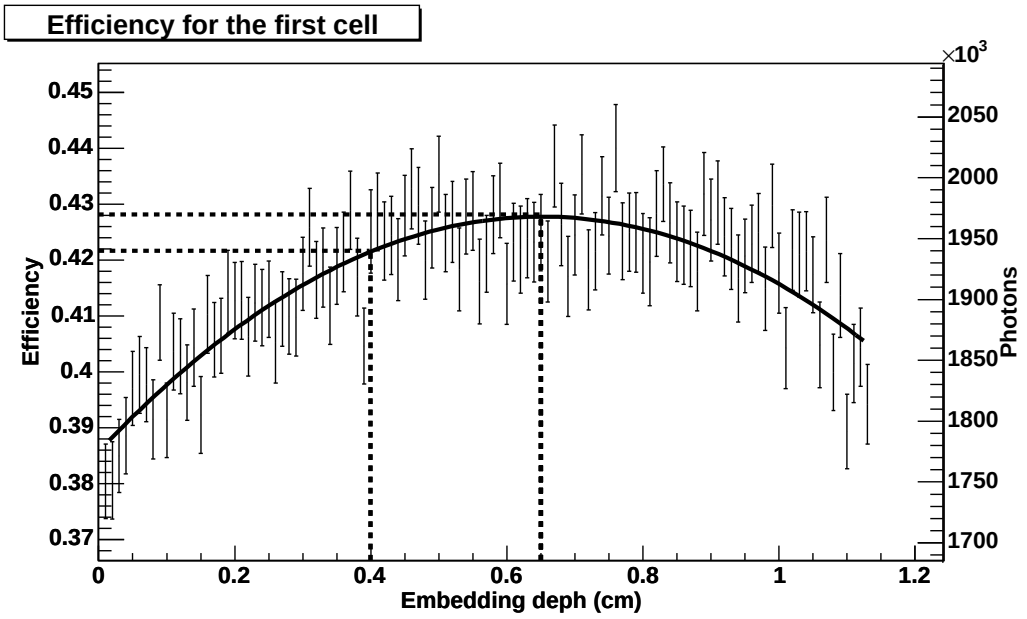

Figure 9: Efficiency vs fiber embedding deph. The right axis correspond to the mean number of photons collected. We draw a second order polinomial fit to show the diferences between the optimal and current values.

3.1.3 Efficiency dependence upon the fiber embedding depth

Figure 9 shows the efficiency versus the fiber embedding depth for the first cell. From this figure, the optimal depth is 6.5 mm, which is compatible with the experimental measurement and with a simple geometrical criteria where fibers would be equally distributed across the plastic cross section. According to that, the optimal depth is located at $\frac{1}{3}$ of the thickness. For technical reasons, however, the construction of V0A used a 4mm embedding deph which, as can be seen in figure 9, is still a good choice.

3.2 Transition to the Photomultiplier Tube

In this section, we simulate the propagation of photons in the WLS fibers all the way up to reach the PMT. As LITRANI does not have a wavelength shifting characterization for materials, we have written our own simulation code assuming the characteristics of WLS materials according to figure 3. The algorithm used and the results obtained are described bellow.

We have used a MonteCarlo routine based on LITRANI scintillating code. That is, if a photon with a certain wavelength goes through a WLS material it will be absorbed with a probability described by the absorption curve. If that happen, it will emit, at the same position but with random direction over 4π, a photon with a wavelength generated randomly in the emission curve distribution. For this, we had to include a parameter related to the penetrability of photons in a WLS material. This parameter measures the mean free

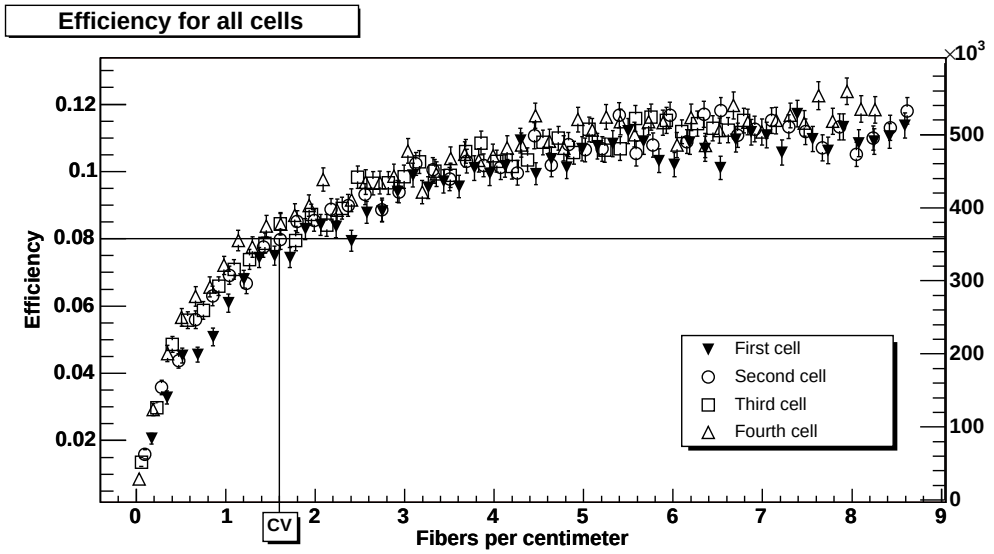

Figure 10: Efficiency vs number of fibers per centimeter including wavelength shifting effect. The right axis correspond to the mean number of photons at PMT.

path for this mechanism, in the same sense as the absorption length for attenuation.

We will assume a 1 meter distance from the outermost cell of the V0A array (cell number four) to the PMT. Then, each cell has fibers with the appropriate lengths to reach the PMT considering their positions in the V0A array. That is, the first cell will have fibers longer than the second; the second, longer that the third; and so on. We shoot one hundred pions randomly according to the description given above. For a density of 1.6 fibers per centimeter, we have approximately 550 thousand photons at the PMT. Figure 10 shows the response of all cells. Note that once again the efficiency curves indicate a flat response in the whole detector.

Figure 11 shows the wavelength and time distributions of the photons generated in the plastic by a 6.5GeV pion. Figure 12 shows the wavelength and time distributions of the photons seen by the PMT. We can see the change of wavelengths due to the fibers and the pulse that reaches the PMT.

The PMT that V0A will use is R5946 from Hamamatsu. We can extract from figure 13 that the quantum efficiency is approximately 20% for the photons we have at the PMT. According to this, we expect a clear signal distributed in time approximately as shown in figure 12.

4 Conclusion

The present simulation represents the first attempt to simulate the transport of scintillating light to the PMT using wavelength shifting fibers. Implementing all the parameters of the V0A, we have validated the design with respect to the uniformity of response, and we have

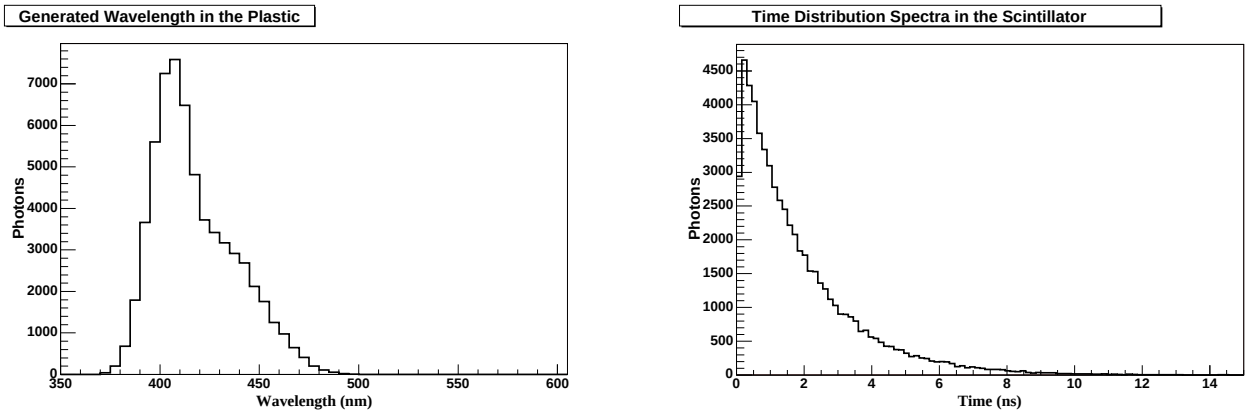

Figure 11: Wavelength and time distributions for the photons generated in the plastic due to one pion for cell 1.

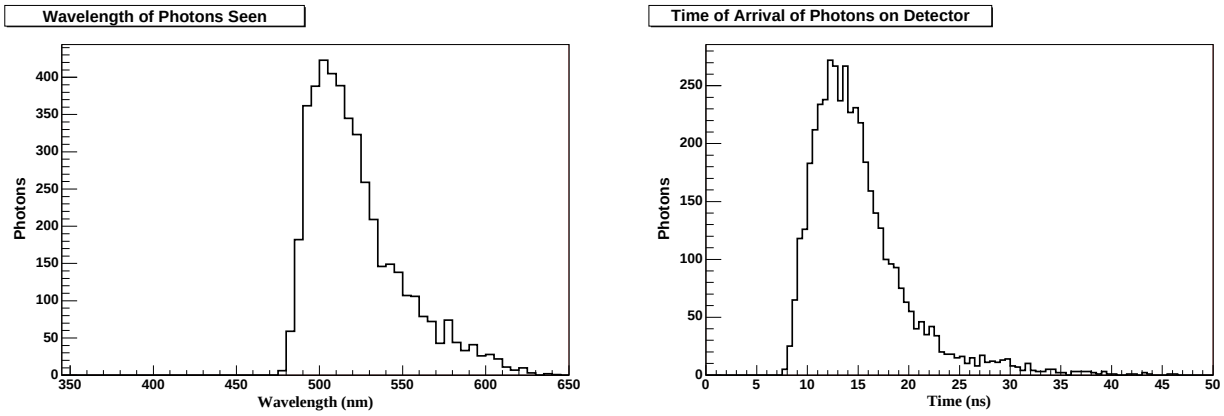

Figure 12: Wavelength and time distributions for the photons detected at PMT due to one pion for cell 1.

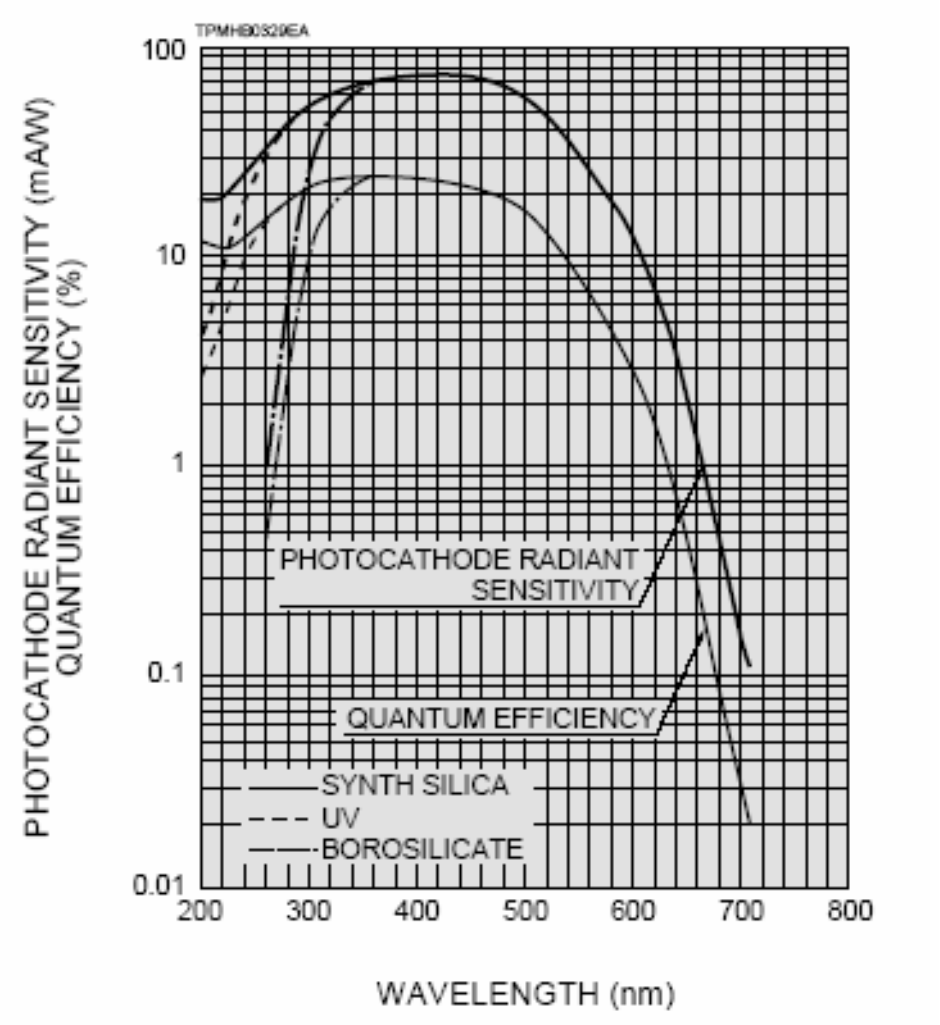

Figure 13: Typical spectral response of the photomultiplier tube. Reproduced from reference [7].

a description of the light pulse shape entering the PMT that could be used for further analysis.

5 Acknowledgements

We wish to thank Dr. G. Contreras, who gave valuable feedback to this work; and Dr. G. Paic, for assistance in the work and useful discussions. This work could not have been possible without the support of DAI-PUCP, HELEN Fellowship and CONACyT.

References

[1] ALICE Collab., *Technical Design Report on Forward Detectors: FMD, T0 and V0*, CERN/LHCC/2004-025

[2] Francois - Xavier Gentit, *LITRANI, Light Transmission for Anisotropic Media*, http://gentit.home.cern.ch/gentit

[3] The ROOT Team, *ROOT, An Object-Oriented Data Analysis Framework*, http://root.cern.ch

[4] BICRON, Saint - Gobain Crystals. *Premium Plastic Scintillators and Scintillating Optical Fibers*, http://www.bicron.com

[5] Particle Data Group. *Review of Particle Physics*, Physics Letters B 592, 1 (2004).

[6] J. B. Birks. *The Theory and Practice of Scintillation Counting*, Pergamon Press, Oxford (1967).

[7] Fine Mesh PMT Series for High Magnetic Field Environments, *Hamamatsu*, http://www.hamamatsu.com